2020 SICE International Symposium on Control Systems (SICE ISCS)
Tokushima University, Tokushima, Japan, March 3-5, 2020

Efficient and life preserving power tracking control of a proton exchange membrane fuel cell using model predictive control

Martin Vrlić[1†], Daniel Ritzberger[2] and Stefan Jakubek[3]

[1]Institute of Mechanics and Mechatronics, University of Technology, Vienna, Austria
(Tel: +43-1-58801-325518; E-mail: martin.vrlic@tuwien.ac.at)
[2]Institute of Mechanics and Mechatronics, University of Technology, Vienna, Austria
(Tel: +43-1-58801-325523; E-mail: daniel.ritzberger@tuwien.ac.at)
[3]Institute of Mechanics and Mechatronics, University of Technology, Vienna, Austria
(Tel: +43-1-58801-325510; E-mail: stefan.jakubek@tuwien.ac.at)

Abstract: In this paper, a method for controlling the operation of a proton exchange membrane fuel cell (PEMFC) stack in an automotive application using model predictive control (MPC) is proposed. As opposed to the conventional way, in which the stoichiometries, pressures or voltage are used as reference values, in this study, the control objective is to fulfill the vehicle power demand while not violating constraints such as exceeding a maximum pressure of cathode and anode, oxygen and hydrogen starvation, etc. which would, if violated, damage the fuel cell stack and thus, shorten its lifetime. With this approach, the MPC drives the pressures, masses and voltage to their optimal values and they do not have to be set by the engineer. A control oriented zero dimensional nonlinear model is used to conduct the research. Simulation analysis of transient power demand trajectories show that this approach can successfully draw the desired power from the fuel cell stack while adhering to various operational constraints.

Keywords: model predictive control, nonlinear systems, automotive control, fuel cell, efficient control, preserve lifetime

1. INTRODUCTION

In the worldwide search for clean sources of energy, the answer may lie in the most abundant element there is available on Earth – hydrogen. Fuel cells use hydrogen as fuel together with oxygen in an electrochemical reaction to produce electric current with water and heat as its byproduct, not contributing to pollution. Among fuel cells there are many different types, but due to their high power density, fast start-up and high efficiency, proton exchange membrane fuel cells (PEMFC) are considered to be the best option to use in an automotive application. In a vehicle, during operation, the power demand which has to be provided by the fuel cell stack, changes rapidly. Such dynamic operating conditions can easily lead to situations such as hydrogen and oxygen starvation, anode-to-cathode over- or underpressure, humidity cycles, etc., all of which cause degradation of the stack. A control system able to satisfy the desired power demand, but at the same time, adhering to life preserving constraints, is crucial for every fuel-cell-powered vehicle. Many studies concerning fuel cell modeling and control have been conducted during the last decade, some of which focus on the cathode or anode side only [1-4], while others examine the behaviour of the whole fuel cell. [5, 6]

The most common control goal in terms of saving the life of the fuel cell found in literature is avoiding starvation which is commonly understood as keeping the stoichiometry at, or above, a certain level. In [2], flatness approach has been used to control the oxygen stoichiometry and cathode pressure. Feedback linearization has been used to track an optimal reference of the oxygen excess ratio for the air supply subsystem of a fuel cell as seen in [7]. Model predictive control (MPC), which is the control scheme used in this work, has also been used in previous research regarding fuel cell operation control. For example, in [8], the problem of oxygen starvation is addressed with keeping the oxygen stoichiometry constant while satisfying the current demand distributing it between the fuel cell and a bank of ultracapacitors using MPC. In addition, keeping the pressure in the fuel cell, along with the stoichiometry at a certain setpoint has also been studied and used in order to prevent starvation [9]. However, controlling the fuel cell in a vehicular operation with a set of reference values for the pressures and stoichiometries is not realistic as the trajectories of the mentioned quantities are generally not known. Instead, it is more plausible to think of a it as a constantly changing demand of power that has to be supplied by the fuel cell. Studies in terms of controlling power demands using MPC have also been done in the past. The work presented in [10] shows an example of tracking the power reference using a nonlinear model predictive controller (NMPC) (applied to a simplified pressure-driven model) divided into three sections: a power controller which calculates the optimal references of the current, pressure of cathode and pressure of anode in order to satisfy the power demand; and 2 lower level controllers which follow the calculated pressure references which implicitly take care of starvation issues. An optimization of the fuel cell model parameters which ensure maximum efficiency when controlling power using MPC is shown in [11], where starvation is avodied by enforcing constraints on the oxygen and hydrogen stoichiometry. Additionally, the temperatures are constrained between certain bounds. Another control goal in avoiding the destruction of the fuel cell and prolonging its durability is the anode-to-cathode overpres-

† Martin Vrlić is the presenter of this paper.

978-4-907764-64-7 © 2020.
The Society of Instrument and Control Engineers
(SICE)

sure control. An MPC was developed for a pneumatic model of a 9-cell Ballard PEM fuel stack in [12] to satisfy a current demand while keeping the overpressure between cathode and anode at 50 mbar.

This work is about the following study analysis and control objectives. Assuming the fuel cell stack is in a vehicular operation, a top-level-controller, based on the driver's actions, provides a reference for the power that has to be delivered by the stack. In this study, the reference is considered to be given. The power demand reference is forwarded to the lower level MPC (the topic of this work) which performs an online optimization and as a result gives the optimal control move in terms of hydrogen and air volume inflows, as well as the cathode backpressure valve position and the current. In order to preserve the lifetime of the fuel cell, avoiding starvation and under-/overpressure is ensured via reactant mass and pressure difference constraints, respectively. The structure of the nonlinear, mass-driven model which is used to run all the simulation tests is presented in Section II. In Section III the controller design and constraints formulation is discussed, while in Section IV the results are presented. Finally, the work is concluded along with indication towards future research in Section V.

2. FUEL CELL MODEL STRUCTURE

In this section, the structure of the model used to conduct the study is presented. The cathode and the anode submodels are represented as three volumes interconnected with nozzles represented by their discharge coefficients, shown in Fig.1. The meaning of each of the volumes is as follows:

- cathode / anode supply manifold
- cathode / anode channel
- cathode / anode exit manifold

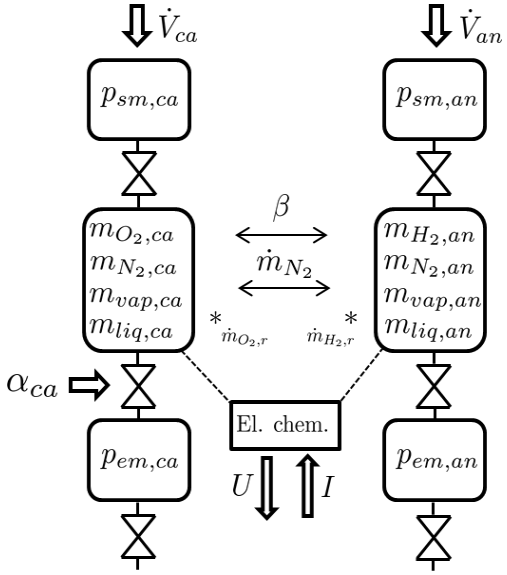

Fig. 1: Fuel cell model structure

The equations that determine the dynamics of the system are: the ideal gas law, the mass balance equation, the linearized nozzle equation and the electrochemical equations based on the work of Kulikovsky [13]. Also, water tansportation through the membrane and nitrogen crossover (marked as β and $\dot{m}_{N_2}$ respectively in Fig.1) are considered. The system operates in a dead end anode mode so hydrogen is not vented out. The model is zero dimensional, meaning that there is no spatial distribution of the states that describe the system along the channel. The reason for choosing such a model lies in its computational efficiency. Combining all the mentioned characteristics, we end up with a nonlinear state-space system of the form:

$$\begin{aligned} \dot{\mathbf{x}} &= \mathbf{f}(\mathbf{x}, \mathbf{u}) \\ \mathbf{y} &= \mathbf{h}(\mathbf{x}, \mathbf{u}), \end{aligned} \tag{1}$$

where $\mathbf{x}$ is the state vector, $\mathbf{u}$ is the input vector and $\mathbf{y}$ is the output vector which has been divided into:

- the variables that have to be constrained to ensure all the safety regulations (constrained variables),
- the variables that are subject to control (controlled variables).

The description of each variable in the state and input vector is given in Table 1 and the description of the output vector variables is given in Table 2. The pressure

Table 1: State and input variables description

State variables	**State description**
$p_{sm,ca}$	Cathode supply manifold pressure
$m_{O_2,ca}$	Oxygen mass in cathode
$m_{N_2,ca}$	Nitrogen mass in cathode
$m_{vap,ca}$	Water vapor mass in cathode
$m_{liq,ca}$	Liquid water mass in cathode
$p_{em,ca}$	Cathode exit manifold pressure
$p_{sm,an}$	Anode supply manifold pressure
$m_{H_2,an}$	Hydrogen mass in anode
$m_{N_2,an}$	Nitrogen mass in anode
$m_{vap,an}$	Water vapor mass in anode
$m_{liq,an}$	Liquid water mass in anode
$p_{em,an}$	Anode exit manifold pressure
Input variables	**Input description**
$\dot{V}_{ca}$	Air volume flow
α_{ca}	Cathode-to-exit manifold backpressure valve position
$\dot{V}_{an}$	Hydrogen volume flow
I	Current

difference across the membrane is approximated as:

$$\Delta p = p_{sm,an} - p_{sm,ca}, \tag{2}$$

the power is defined as:

$$P = U \cdot I, \tag{3}$$

and the power loss is defined as:

$$P_{loss} = E_0 \cdot I - P \tag{4}$$

with E_0 being the open circuit voltage.

Table 2: Output variables description

Constrained	**Output description**
$m_{O_2,ca}$	Oxygen mass in cathode
$m_{H_2,an}$	Hydrogen mass in anode
$p_{sm,ca}$	Cathode supply manifold pressure
$p_{sm,an}$	Anode supply manifold pressure
Δp	Pressure difference across membrane
Controlled	**Output description**
P	Power
P_{loss}	Power loss

3. CONTROL DESIGN

The control goal is to satisfy the transient power demand keeping the power loss as small as possible while adhering to various fuel-cell-life-preserving constraints. The model is linearized around an operating point and discretized with the sampling time of 10 miliseconds and the MPC is designed for the newly obtained discrete linear system. Afterwards, the linear MPC is applied to the nonlinear system and in the vicinity of the operating point ($\pm$ 10% deviation), a transient power demand can be successfully fulfilled. The operating point can be chosen arbitrarily as the linearization is done analytically. By doing so, every part of the operating region can be controlled with its own linear MPC.

3.1. Model linearization

For model linearization, an appropriate operating point is necessary. In this subsection, the choice and formulation of an operating point will be discussed.
Choosing a constant input vector $\mathbf{u}_0$, setting the state vector to be constant ($\dot{\mathbf{x}} = \mathbf{0}$), and solving the state and output equation of the nonlinear system in Eq. (1), we obtain the state and output vector for which the system is in stationary operation denoted as $\mathbf{x}_0$ and $\mathbf{y}_0$, respectively. The choice of the operating point depends on the part of the operating region that needs to be examined. For example, if starvation effects are to be examined, then the air and hydrogen volume flows will be set to a relatively low value; for the point in the vicinity of maximum power, a higher current density will be chosen, etc.
After choosing an operating point, a linearized state space model of the form

$$\begin{aligned} \dot{\widetilde{\mathbf{x}}} &= \mathbf{A}\,\widetilde{\mathbf{x}} + \mathbf{B}\,\widetilde{\mathbf{u}}, \\ \widetilde{\mathbf{y}} &= \mathbf{C}\,\widetilde{\mathbf{x}} + \mathbf{D}\,\widetilde{\mathbf{u}}, \end{aligned} \tag{5}$$

is obtained where $\widetilde{\mathbf{x}} = \mathbf{x} - \mathbf{x}_0$, $\widetilde{\mathbf{u}} = \mathbf{u} - \mathbf{u}_0$ and $\widetilde{\mathbf{y}} = \mathbf{y} - \mathbf{y}_0$ are the deviations from the operating point. The matrices **A**, **B**, **C** and **D** are defined in Eq. (6):

$$\begin{aligned} \mathbf{A} &= \left.\frac{\partial \mathbf{f}(\mathbf{x},\mathbf{u})}{\partial \mathbf{x}}\right|_{op}, & \mathbf{B} &= \left.\frac{\partial \mathbf{f}(\mathbf{x},\mathbf{u})}{\partial \mathbf{u}}\right|_{op}, \\ \mathbf{C} &= \left.\frac{\partial \mathbf{h}(\mathbf{x},\mathbf{u})}{\partial \mathbf{x}}\right|_{op}, & \mathbf{D} &= \left.\frac{\partial \mathbf{h}(\mathbf{x},\mathbf{u})}{\partial \mathbf{u}}\right|_{op}, \end{aligned} \tag{6}$$

where *op* denotes the operating point $(\mathbf{x}_0, \mathbf{u}_0, \mathbf{y}_0)$.

3.2. Model discretization

Using zero order hold discretization, the continuous time linear model shown in Eq.(5) is turned into a discrete time linear system shown in Eq.(7) with a sampling time of 10 miliseconds.

$$\begin{aligned} \widetilde{\mathbf{x}}(k+1) &= \mathbf{A}_m\widetilde{\mathbf{x}}(k) + \mathbf{B}_m\widetilde{\mathbf{u}}(k), \\ \widetilde{\mathbf{y}}(k) &= \mathbf{C}_m\widetilde{\mathbf{x}}(k) + \mathbf{D}_m\widetilde{\mathbf{u}}(k), \end{aligned} \tag{7}$$

With the discrete time model acquired, the prerequisites for designing an MPC are met.

3.3. MPC cost function

Solving a problem using MPC is essentially calculating the optimal control move in order to achieve a desired goal with minimal effort using the prediction of future events based on the model. In the context of this study, the "effort" is the action of all the actuators $\mathbf{u} = [\dot{V}_{ca} \quad \alpha_{ca} \quad \dot{V}_{an} \quad I]^{\mathrm{T}}$. Let's define the increment of the control variable at time $k + j$,

$$\Delta\widetilde{\mathbf{u}}(k+j) = \widetilde{\mathbf{u}}(k+j) - \widetilde{\mathbf{u}}(k+j-1), \tag{8}$$

The optimization itself is done by means of minimizing a cost function (Eq. (9)) with $\Delta\widetilde{\mathbf{u}}(k+j)$ as its decision variables:

$$\begin{aligned} J = &\sum_{i=1}^{N_p} ||\widetilde{\mathbf{y}}_{ref}(k+i) - \hat{\widetilde{\mathbf{y}}}(k+i)||^2_{\boldsymbol{\mathcal{Q}}_{\mathbf{y}}} + \\ &+ \sum_{j=0}^{N_c-1} ||\Delta\widetilde{\mathbf{u}}(k+j)||^2_{\boldsymbol{\mathcal{R}}} + \sum_{j=0}^{N_c-1} ||\widetilde{\mathbf{u}}(k+j)||^2_{\boldsymbol{\mathcal{R}}_{\mathbf{u}}} \end{aligned} \tag{9}$$

As seen in Table 2, the output vector has been divided

Table 3: Cost function variables description

N_p	prediction horizon
N_c	control horizon
$\hat{\widetilde{\mathbf{y}}}(k+i)$	future predicted outputs
$\widetilde{\mathbf{y}}_{ref}(k+i)$	future reference values
$\Delta\widetilde{\mathbf{u}}(k+j)$	future control increments
$\widetilde{\mathbf{u}}(k+j)$	future input values
$\boldsymbol{\mathcal{Q}}_{\mathbf{y}}$	diagonal weighting matrix for tracking the control error
$\boldsymbol{\mathcal{R}}$	diagonal weighting matrix for control increment costs
$\boldsymbol{\mathcal{R}}_{\mathbf{u}}$	diagonal weighting matrix for input variables costs

into the constrained variables and the controlled variables:

$$\begin{aligned} \mathbf{y}_{constr} = [&m_{O_2,ca} \quad m_{H_2,an} \quad p_{sm,ca} \ldots \\ &\ldots p_{sm,an} \quad \Delta p]^{\mathrm{T}}, \\ \mathbf{y}_{control} = [&P \quad P_{loss}]^{\mathrm{T}}, \end{aligned}$$

so the $\boldsymbol{\mathcal{Q}}_{\mathbf{y}}$ matrix will contain weights for tracking the control error for only the controlled outputs, namely, the power demand that is to be tracked and the power loss that is to be minimized.

3.4. Constraints

One of the strengths of MPC is its ability to cope with constraints, which, in the context of this work, translate to a series of safety limits imposed to the system in order to prevent it from operating in a self-destructive manner. *Pressure related constraints:*

Increasing the efficiency of the fuel cell would also mean increasing the pressures in the cathode and anode and in case their values would exceed a critical point, the stack would be irreversibly damaged. Because in a real system the pressure sensors are usually located at the cathode and anode inlet, the constraints are not imposed on the cathode and anode pressures directly, but rather on the pressures in the supply manifolds. According to the manufacturer of the fuel cell stack for which the model has been parametrized, the safety limits for the cathode and anode supply manifold pressures are as defined in Eqs. (10) and (11).

$$1\ bar \leq\ p_{sm,ca} \leq\ 2\ bar \tag{10}$$

$$1\ bar \leq\ p_{sm,an} \leq\ 2\ bar \tag{11}$$

Also, a constraint for the pressure difference accross the membrane is defined in Eq. (12), as its violation would also destroy the fuel cell stack:

$$0.2\ bar \leq\ \Delta p \leq\ 0.7\ bar. \tag{12}$$

Starvation related constraints:

Starvation in fuel cells is usually explained as having the hydrogen or oxygen stoichiometry lower than 1, meaning that the reactant mass that gets consumed is not fully compensated by the inflow. However, that does not mean that the system does not have enough reactants to continue with the operation for a certain amount of time, even if the stoichiometry is below 1. Strictly speaking, starvation would indicate the depletion of hydrogen and oxygen. For that reason, in this paper, starvation is not avoided by setting a constraint on the stoichiometries, but rather on the masses of hydrogen and oxygen inside the anode and cathode manifolds, respectively. The idea behind choosing a suitable lower safety limit for the reactant masses is simply considering the fact that there is a certain delay of the inflow gases from their source to the spot where they will be consumed due to compressor dynamics or if the inflows are cut off for some unpredicted reason, so during that time, the consumption of hydrogen and oxygen cannot be fully compensated. It is then necessary to make sure that there is enough hydrogen and oxygen mass left for the reaction to take place during that time interval in which the compensation is not possible. Let's denote the time interval for which we want to have a safety reserve as T_{safe} and the moment in which the inflow is cut off as t. The consumed mass of hydrogen and oxygen during that time is shown in Eqs. (13) and (14), respectively,

$$\Delta m_{H_{2,consumed}} = \int_{t}^{t+T_{safe}} \frac{I(\tau)}{2F} \cdot M_{H_2} \cdot N_{cells}\, d\tau, \tag{13}$$

$$\Delta m_{O_{2,consumed}} = \int_{t}^{t+T_{safe}} \frac{I(\tau)}{4F} \cdot M_{O_2} \cdot N_{cells}\, d\tau, \tag{14}$$

where I is the drawn current, set by the engineer for calculating the appropriate safety limit, N_{cells} is the number of cells in the stack, F is the Faraday constant and M_{H_2} and M_{O_2} are the molar masses of hydrogen and oxygen, respectively. In order to always have a reserve for a chosen safety time, the constraints on the hydrogen and oxygen mass are then:

$$m_{H_2} \geq \Delta m_{H_{2,consumed}} \tag{15}$$

$$m_{O_2} \geq \Delta m_{O_{2,consumed}} \tag{16}$$

4. RESULTS AND DISCUSSION

In this section, the simulation results of tracking a transient power demand while adhering to constraints and minimizing the power loss are presented. For all the simulation tests, the prediction horizon is $N_p = 100$ samples (1 second) and the control horizon is $N_c = 30$ samples (0.3 seconds).

4.1. Power demand tracking with starvation management

In this subsection, simulation tests which demonstrate the ability of the MPC to manage situations in which starvation would occur are presented. The results are brought forth as a comparison between the fuel cell operation when the constraints are not imposed on the system versus the operation in which they are. Power loss minimization is not considered in the tests presented in this subsection so the $\mathcal{Q}_\mathbf{y}$ matrix will contain a nonzero weight only for tracking the power demand (Eq.(17)). Simulation tests with consideration of power losses will be discussed in Subsection 4.2

$$\mathcal{Q}_\mathbf{y} = \begin{bmatrix} 1 & 0 \\ 0 & 0 \end{bmatrix} \tag{17}$$

The power trajectory tracked by the MPC is shown in Fig. 2 and to increase readability, the step at time $t = 5s$ is shown in Fig. 3 from which the predictive behaviour of the controller is obvious. Also, there is no offset from the reference value when the power settles for both the unconstrained and constrained case. If we decide that we

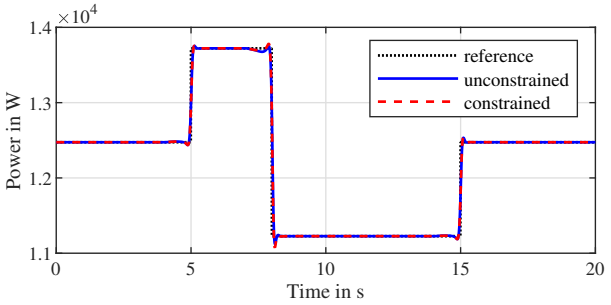

Fig. 2: Power demand tracking - unconstrained vs. constrained

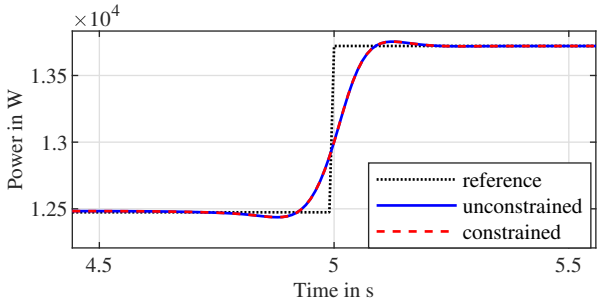

Fig. 3: Power demand tracking - unconstrained vs. constrained - step at $t = 5s$

want to have at least $2 \cdot 10^{-4} kg$ of oxygen in the cathode for reserve, then a constraint on the oxygen mass inside the cathode will be implemented into the MPC. Simulation tests in Fig. 4 show that tracking the power demand from Fig. 2 in the unconstrained case would lead to oxygen mass dropping below the safety line of $2 \cdot 10^{-4} kg$, but if the constraint is taken into account, then the controller will keep the oxygen mass above the limit, as seen on the same figure. Comparing the behaviour of each of the actuators shown on Figs. 5 and 6 for the unconstrained and constrained case, it can be seen that, in order to keep the oxygen mass above the limit, the air flow in Fig. 5 is kept at a higher value in the constrained case and the current in Fig. 6 is a little reduced in the constrained case for the power to be still successfully tracked. Due to their low influence on adjusting the oxygen mass, the nozzle opening and hydrogen flow have negligible difference in the constrained and unconstrained case, so those plots have been ommited. For all simulations, the weighting matrices $\boldsymbol{\mathcal{R}}$ and $\boldsymbol{\mathcal{R}_u}$ are:

$$\boldsymbol{\mathcal{R}} = \begin{bmatrix} 1 & 0 & 0 & 0 \\ 0 & 1 & 0 & 0 \\ 0 & 0 & 1 & 0 \\ 0 & 0 & 0 & 1 \end{bmatrix}, \boldsymbol{\mathcal{R}_u} = \begin{bmatrix} 0 & 0 & 0 & 0 \\ 0 & 1 & 0 & 0 \\ 0 & 0 & 0 & 0 \\ 0 & 0 & 0 & 0 \end{bmatrix} \tag{18}$$

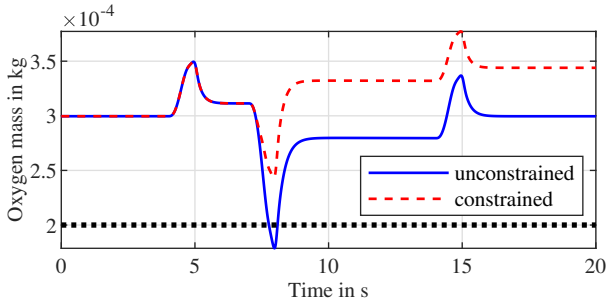

Fig. 4: Oxygen mass in cathode - unconstrained vs. constrained

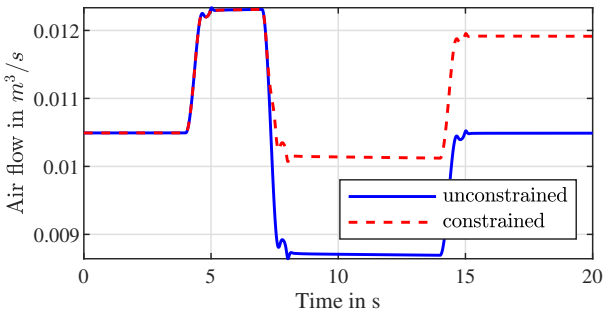

Fig. 5: Air flow - unconstrained vs. constrained

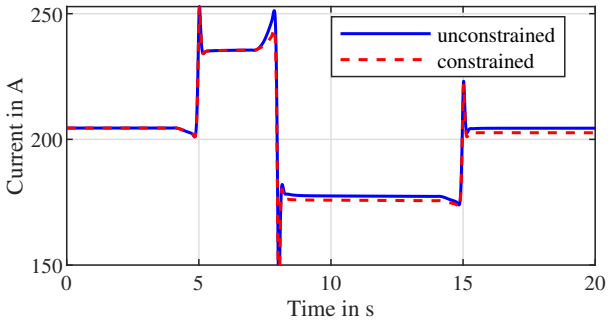

Fig. 6: Current - unconstrained vs. constrained

4.2. Power demand tracking with minimal power loss

In addition to preserving the life of the fuel cell stack, it is also important to operate it in an efficient mode. In this study, efficiency is understood as making the power losses defined in Eq. (4) as small as possible. MPC wise, the weighting factor for penalizing the power loss in the $\boldsymbol{\mathcal{Q}}_\mathbf{y}$ matrix will be nonzero so the matrix itself will be:

$$\boldsymbol{\mathcal{Q}}_\mathbf{y} = \begin{bmatrix} 10 & 0 \\ 0 & 0.01 \end{bmatrix}. \tag{19}$$

In this subsection, a comparison between the efficient and nonefficient operation is presented. For all simulations, the weighting matrices $\boldsymbol{\mathcal{R}}$ and $\boldsymbol{\mathcal{R}_u}$ are:

$$\boldsymbol{\mathcal{R}} = \begin{bmatrix} 1 & 0 & 0 & 0 \\ 0 & 1000 & 0 & 0 \\ 0 & 0 & 1 & 0 \\ 0 & 0 & 0 & 100 \end{bmatrix}, \boldsymbol{\mathcal{R}_u} = \begin{bmatrix} 0 & 0 & 0 & 0 \\ 0 & 1 & 0 & 0 \\ 0 & 0 & 0 & 0 \\ 0 & 0 & 0 & 0 \end{bmatrix} \tag{20}$$

The controller tracks the power reference steps as shown in Fig. 7. with the step at time $t = 5s$ shown in Fig. 8. Next, comparing the power trajectory in the efficient and nonefficient case, it can be seen that there is a small offset from the reference in the efficient operation because there is a trade-off in the cost function between tracking the power reference and keeping the power loss at minimum. In Fig. 9 the power loss is shown in both cases and the obvious reduction of losses of up to 1000 Watts is worth the imperfect power demand tracking. In order to understand what is happening in the system, it is necessary to examine the controller's performance and the

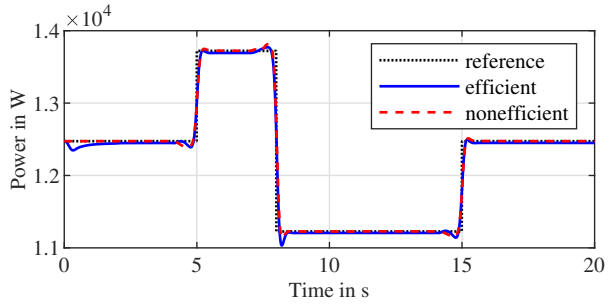

Fig. 7: Power demand tracking - nonefficient vs. efficient

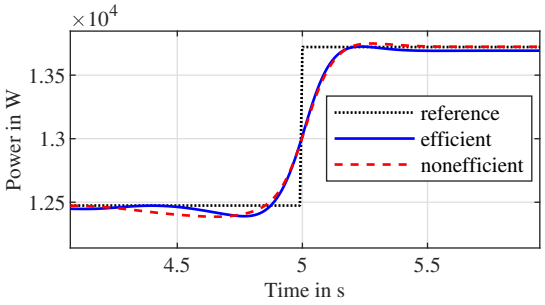

Fig. 8: Power demand tracking - nonefficient vs. efficient - step at $t = 5s$

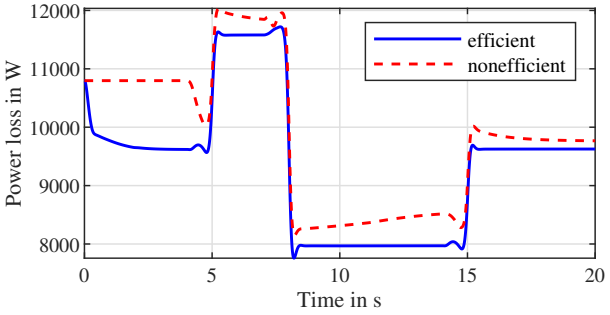

Fig. 9: Power loss - nonefficient vs. efficient

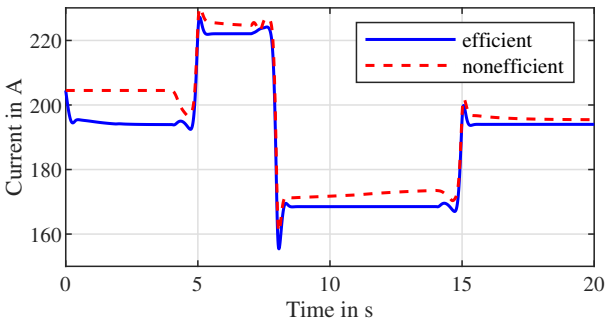

Fig. 10: Current - nonefficient vs. efficient

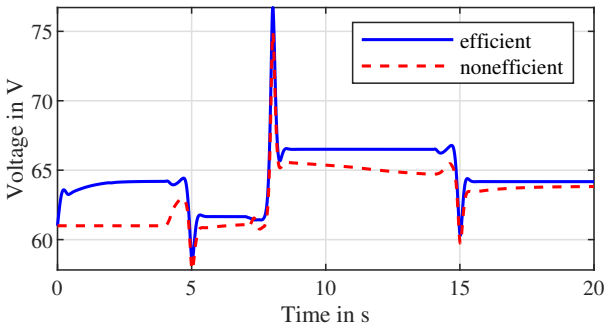

Fig. 11: Voltage - nonefficient vs. efficient

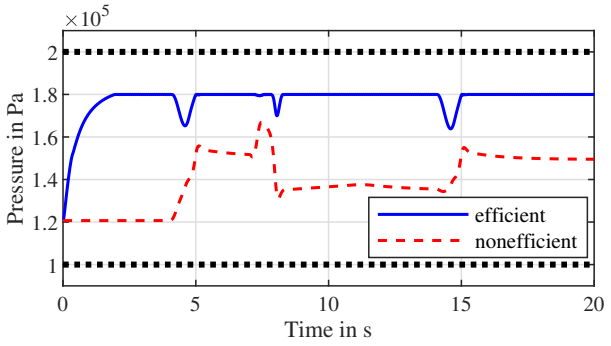

Fig. 12: Cathode supply manifold pressure - nonefficient vs. efficient

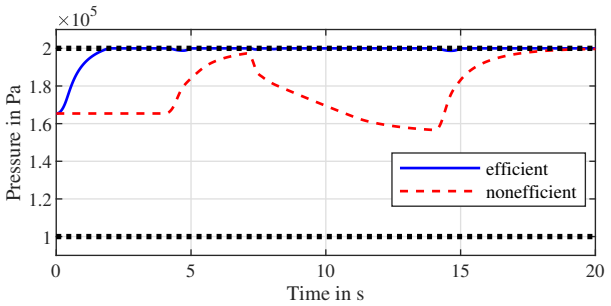

Fig. 13: Anode supply manifold pressure - nonefficient vs. efficient

requirements for which the power loss would be minimized. The power is the product of current and voltage $P = U \cdot I$ so in order to have a power increase, the controller chooses, as the result of optimization, whether it will put more emphasis on increasing the current or in increasing the voltage. In the case where efficiency is not considered, the current is increased more strongly than in the case where efficiency is taken into account, as visible in Fig. 10 which in turn, means that the voltage is more increased in the efficient case as seen in Fig. 11. However, unlike the current, the voltage cannot be directly manipulated so the other three inputs ($\dot{V}_{ca}$, α_{ca} and $\dot{V}_{an}$) have to be used by the controller to adapt the voltage to have minimal power losses. As it turns out, the required voltage increase translates to the controller trying to maximize the pressures in the cathode and anode supply manifolds as is seen in Figs. 12 and 13. Because of the safety limits Eqs. (10, 11), the pressures do not go towards infinity, but obey the constraints. Even though the maximum allowed presssure in the cathode supply manifold pressure is 2 bar, it does not exceed 1.8 bar because there is also the pressure difference constraint active Eq. (12) which states that the pressure on the anode side has to be at least 200 mbar higher than on the cathode side. The pressure difference can be seen in Fig. 14. The behaviour

of the air flow in the efficient case shown in Fig. 15, is trivally explainable by the fact that it settles at the point for which the cathode supply manifold pressure remains at its maximum allowed value - 1.8 bar. To understand the behaviour of the hydrogen flow in the efficient case (Fig. 16), it is necessary to recall that the anode is closed and there is no ouflow of hydrogen. Because of the efficiency requirement, the flow initially rises to increase the pressure, but, if it would stay at its maximum point, the pressure would keep rising and violate its constraint and that is the reason why the flow decreases. Eventually, it settles at the point for which it matches the consumption of hydrogen so the anode supply manifold pressure can stay at 2 bar. Because of the high weight on the nozzle opening visible in Eq. (20), it does little to no action so that plot has been ommited.

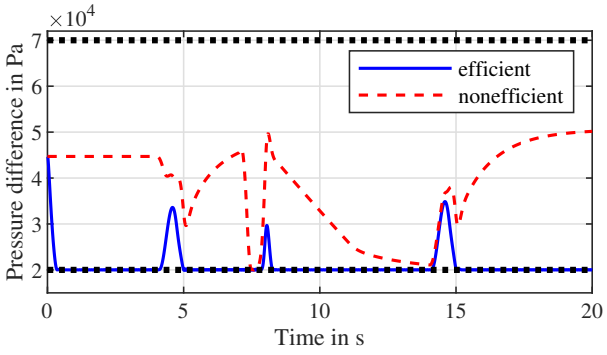

Fig. 14: Pressure difference across membrane - nonefficient vs. efficient

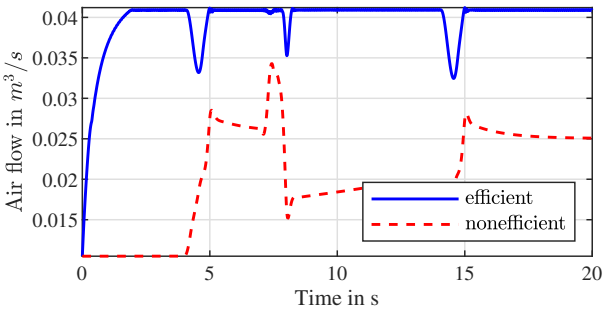

Fig. 15: Air volume flow - nonefficient vs. efficient

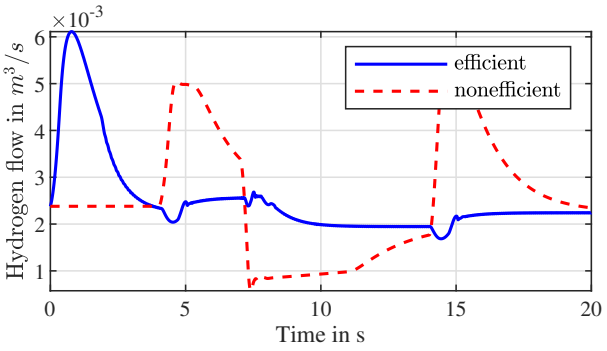

Fig. 16: Hydrogen volume flow - nonefficient vs. efficient

5. CONCLUSION

In this paper, efficient and life preserving power control of a proton exchange membrane fuel cell in dead end anode mode has been presented. The nonlinear model used for this study is a zero dimensional one having the cathode and anode pressures as well as the oxygen, hydrogen, nitrogen and water masses as states which describe the system. The control itself has been performed using a linear model predictive controller on the nonlinear system. Mass and pressure constraints are imposed to the system to prevent starvation and fuel cell destruction. Efficient operation has also been considered in terms of power loss minimization. Satisfactory results have been observed as the linear MPC shows good performance in the range of $\pm 10\%$ deviation from the linearization point. Future work involves development of an MPC capable of controlling the system outside the $\pm 10\%$ range as well as a state estimator.

ACKNOWLEDGMENT

The results presented in this work are the fruit of one of the many research projects funded by the Austrian Research Promotion Agency (FFG): "Performance-Recovery Strategy & Advanced Control for Efficient Fuel Cell Operation" (PROTECT)

REFERENCES

[1] M.A. Danzer, J. Wilhelm, H. Aschemann and E. P. Hofer, "Model-based control of cathode pressure and oxygen excess ratio of a PEM fuel cell system", *Journal of Power Sources*, Vol. 176, No. 2, pp. 515–522, 2008.

[2] R. da Fonseca et al., "Control of PEMFC system air group using differential flatness approach: Validation by a dynamic fuel cell system model", *Applied Energy*, Vol. 113, pp. 219–229, 2014.

[3] J. Chen, Z. Liu, F. Wang, Q. Ouyang and H. Su, "Optimal Oxygen Excess Ratio Control for PEM Fuel Cells",
IEEE Transactions on control systems technology, Vol. 26, No. 5, pp. 1711–1721, 2018.

[4] A. Ebadighajari, J. De Vaal and F. Golnaraghi, "Multivariable Control of Hydrogen Concentration and Fuel Over-Pressure in a Polymer Exchange Membrane Fuel Cell with Anode Re-circulation",
American Control Conference (ACC), 2016.

[5] J.T. Pukrushpan, A.G. Stephanopoulou and H. Peng, "Control of Fuel Cell Power Systems: Principles, Modeling, Analysis and Feedback design", *Advances in Industrial Control*, Springer-Verlag, 2004.

[6] Q. Li, W. Chen, Y. Wang, J. Jia and M. Han, "Nonlinear robust control of proton exchange membrane fuel cell by state feedback exact linearization", *Journal of Power Sources*, Vol 194. pp. 338–348, 2009.

[7] Z. Liu, J. Chen, H. Chen and C. Yan, "Air supply regulation for PEMFC systems based on uncertainty and disturbance estimation",

International Journal of Hydrogen Energy, Vol. 43, No. 25, pp. 11559–11567, 2018.

[8] A. Vahidi, A. Stefanopoulou and H. Peng, "Current Manegement in a Hybrid Fuel Cell Power System: A Model-Predictive Control Approach", *IEEE Transactions on control systems technology*, Vol. 14, No. 6, pp. 1047–1057, 2006.

[9] M. A. Danzer, S. J. Wittmann and E. P. Hofer, "Prevention of fuel cell starvation by model predictive control of pressure, excess ratio, and current", *Journal of Power Sources*, Vol. 190, No.1 pp. 86–91, 2009.

[10] C. Hähnel, V. Aul, J. Horn, "Power Control for Efficient Operation of a PEM Fuel Cell System by Nonlinear Model Predictive Control", *IFAC-PapersOnLine*, Vol. 48, No. 11 pp. 174–179, 2015.

[11] V. Meidanshahi, G. Karimi, "Dynamic modeling, optimization and control of power density in a PEM fuel cell", *Applied Energy*,Vol. 93, pp. 98–105, 2012.

[12] A. Ebadighajari, J. De Vaal, F. Golnaraghi, "Optimal Control of Fuel Over-Pressure in a Polymer Electrolyte Membrane Fuel Cell System during Load Change", *IEEE American Control Conference*, pp. 3236-3241, 2015.

[13] A. A. Kulikovsky, "The voltage–current curve of a polymer electrolyte fuel cell: "exact" and fitting equations", *Electrochemistry Communications*, Vol. 4, pp. 845–852, 2002.